NANO LETTERS

2007
Vol. 7, No. 12
3569−3575

Simple Approach for High-Contrast Optical Imaging and Characterization of Graphene-Based Sheets

Inhwa Jung,[†] Matthew Pelton,[‡] Richard Piner,[†] Dmitriy A. Dikin,[†] Sasha Stankovich,[†] Supinda Watcharotone,[†] Martina Hausner,[§] and Rodney S. Ruoff*,[†]

Department of Mechanical Engineering, Northwestern University, Evanston, Illinois 60208, Center for Nanoscale Materials, Argonne National Laboratory, Argonne, Illinois 60439, and Department of Chemistry and Biology, Ryerson University, 350 Victoria Street, Toronto, Ontario M5B 2K3, Canada

Received June 13, 2007; Revised Manuscript Received September 3, 2007

ABSTRACT

A simple optical method is presented for identifying and measuring the effective optical properties of nanometer-thick, graphene-based materials, based on the use of substrates consisting of a thin dielectric layer on silicon. High contrast between the graphene-based materials and the substrate is obtained by choosing appropriate optical properties and thickness of the dielectric layer. The effective refractive index and optical absorption coefficient of graphene oxide, thermally reduced graphene oxide, and graphene are obtained by comparing the predicted and measured contrasts.

Identifying and characterizing a single nanometer-scale layer, or a small number of layers, of materials such as graphite, any of a number of clays, or metal dichalcogenides such as WS_2, is challenging yet critical for the study of such materials.[1,2] Scanning probe microscopy methods, such as atomic force microscopy (AFM), can both identify the presence of such thin sheets and determine their lateral and vertical dimensions.[3] Because these methods are time consuming at the resolution required to discriminate between single and bilayers of a material, the scan area must be restricted. Scanning electron microscopy can also, in principle, be used for identification of individual layers versus multilayer sheets, but this imaging typically induces the formation of a layer of contaminant in the exposed region.[4]

Optical methods, on the other hand, offer the potential for rapid, nondestructive characterization of large-area samples. Ellipsometry, for example, is widely used to determine the optical constants and thicknesses of thin films. Standard ellipsometers, though, require samples with lateral dimensions well over a millimeter. By contrast, imaging ellipsometry can have submicrometer resolution and may be useful for probing optical constants and thicknesses.[5,6] Investigations into this method are ongoing and will be reported elsewhere. For the past two years, we have focused on simpler methods that allow the use of standard confocal microscopy for rapid identification and characterization of the optical response of thin sheets.[7,8]

In particular, we have investigated the use of substrates designed to interferometrically enhance the visibility of thin sheets. Interference techniques have been used for over half a century to allow for the imaging of low-contrast and transparent samples.[9,10] Over the past decade, microscopy of fluorescent monolayers has been enhanced by incorporating a thin dielectric layer between the material and a reflective substrate.[11] Fabry-Perot interference in the dielectric layer modulates the fluorescence intensity, allowing the determination of the thicknesses of surface layers with nanometer precision.[12] Recently, a similar method has been used for the identification of single graphene sheets.[1,2] Graphene monolayers and multilayers were deposited on substrates consisting of a silicon wafer with an intermediate, 300 nm thick silicon dioxide layer, and the monolayers were qualitatively identified by their weak contrast under white light illumination. The contrast between the graphene layers and the substrate has been modeled using a multilayer interference method.[13,14] It was thereby shown that contrast could be improved by using narrow band illumination, thereby allowing for the straightforward determination of the number of graphene layers.[15,16] Spectral resolution of the

* Corresponding author. Tel: (847) 467-6596. Fax: (847) 491-3915. E-mail: r-ruoff@northwestern.edu.
[†] Northwestern University.
[‡] Argonne National Laboratory.
[§] Ryerson University.

10.1021/nl0714177 CCC: $37.00
Published on Web 11/02/2007

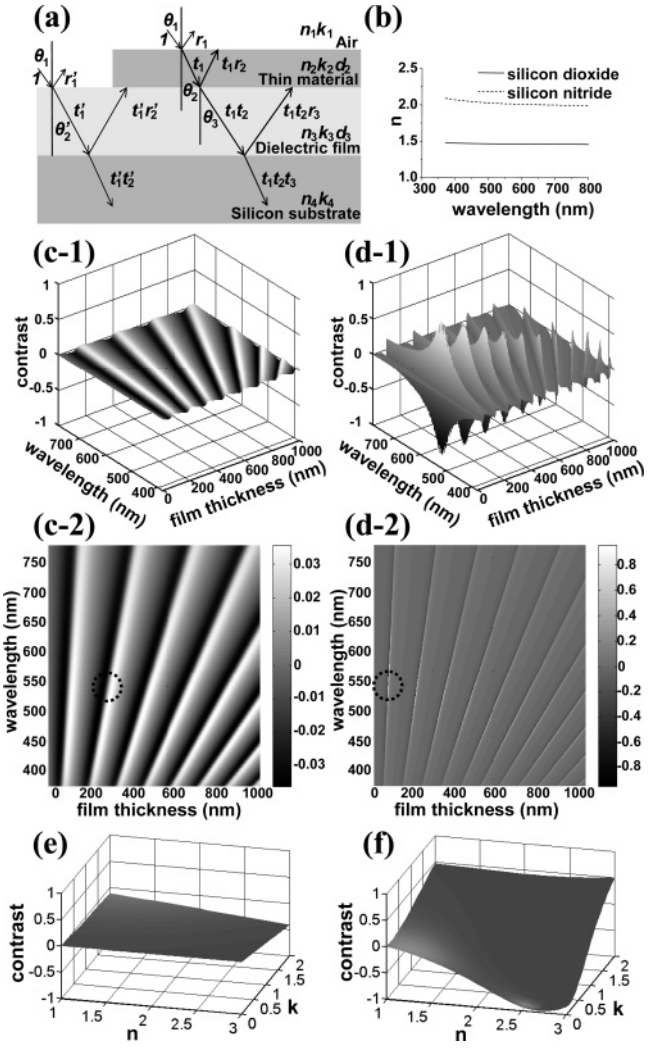

Figure 1. (a) Optical reflection and transmission for layered thin-film system: dielectric film on silicon substrate (left), thin sheet added on dielectric film (right). (b) Index of refraction of silicon dioxide (solid line) and stoichiometric silicon nitride (dashed line). (c,d) Contrast as a function of wavelength and film thickness for (c) silicon dioxide layer and (d) silicon nitride layer, each on Si. Calculated contrast dependence on the material refractive index, *n*, and optical absorption coefficient, *k*, for (e) a 275 nm thick silicon dioxide layer and (f) a 64.5 nm thick silicon nitride layer, assuming an optical wavelength of 543 nm and a numerical aperture of illumination of 0.29.

contrast was used for approximate determination of the optical properties of graphene layers.[17] However, limited contrast was observed for single layers, with the reflectivity from the thin sheet at most 10% less than the reflectivity from the bare substrate. Here, we show that the substrate can be optimized to provide for much higher-contrast imaging, allowing reflectivity from single layers to be more than 12 times that from the bare substrate. The high visibility allows for systematic comparison of observed contrast to the calculations leading to a quantitative determination of the effective optical properties of the thin sheets on the substrates.

The thin sheets that we focus on in this study are graphite oxide layers. Graphite oxide is a layered material that can readily be exfoliated to form stable colloidal suspensions in water.[18,19] At an appropriate concentration, evaporation of droplets of such a colloidal suspension on a surface yields almost exclusively individual layers, hereafter referred to as graphene oxide. According to our own measurement, graphene oxide is not electrically conductive and its optical properties are thus expected to differ markedly from those of graphite. We have found that the electrical conductivity of individual layers of graphene oxide can be increased by heating them in vacuum or through appropriate chemical reduction, making it a material of interest for electrical devices.[20] As we show here, the thermal treatment of the graphene oxide layers also alters their effective optical properties.

To optimize the substrate, we have calculated the expected contrast between light reflected from the sample with and without the graphene oxide layer. Figure 1a shows a schematic of optical reflection and transmission for the layered thin-film system. For a dielectric film on a substrate (here, Si), the system has two interfaces; with the addition of the graphene oxide layer, a third interface is added. Because a portion of the beam is reflected from each interface and the rest is transmitted, an infinite number of optical paths are possible. The amplitude of the reflected beam is a result of interference between all these paths and is determined by the wavelength of the incident beam, λ; its incident angle, θ; the refractive indices, n, of the layers; their absorption coefficients, k; and the layer thicknesses, d.[21,22] In this model, we treat the graphene oxide sheet as a thin slab of material with a certain refractive index and absorption coefficient. These properties are expected to be different from an isolated sheet of material in vacuum and from those of bulk graphene oxide due to the possible presence of adsorbates and local field effects.

The total amplitude of reflected light depends on the phase changes across the thin material ($\delta_2 = d_2(n_2 - ik_2)\cos 2\pi\theta_2/\lambda$) and the dielectric layer ($\delta_3 = d_3(n_3 - ik_3)\cos 2\pi\theta_3/\lambda$), as well as the amplitudes of the light reflected at the three interfaces, between air and the thin layer of material (r_1), between the thin layer of material and the dielectric layer (r_2), and between the dielectric layer and the silicon layer (r_3):

$$r_{\text{platelet}} = \frac{r_1 + r_2\exp(-2i\delta_2) + [r_1r_2 + \exp(-2i\delta_2)]r_3\exp(-2i\delta_3)}{1 + r_1r_2\exp(-2i\delta_2) + r_3\exp(-2i\delta_3)[r_2 + r_1\exp(-2i\delta_2)]} \quad (1)$$

In the absence of the thin layer, the total reflected amplitude is expressed in terms of the phase change across the dielectric layer ($\delta_2' = d_3(n_3 - ik_3)\cos 2\pi\theta_2'/\lambda$) and the amplitudes of the light reflected at the two interfaces, between air and the dielectric layer (r_1') and between the dielectric layer and the silicon layer (r_2'):

$$r_{\text{dielectric}} = \frac{r_1' + r_2'\exp(-2i\delta_2')}{1 + r_1'r_2'\exp(-2i\delta_2')} \quad (2)$$

The reflected intensity can be obtained by multiplying the reflected beam amplitude by its complex conjugate.[23] The

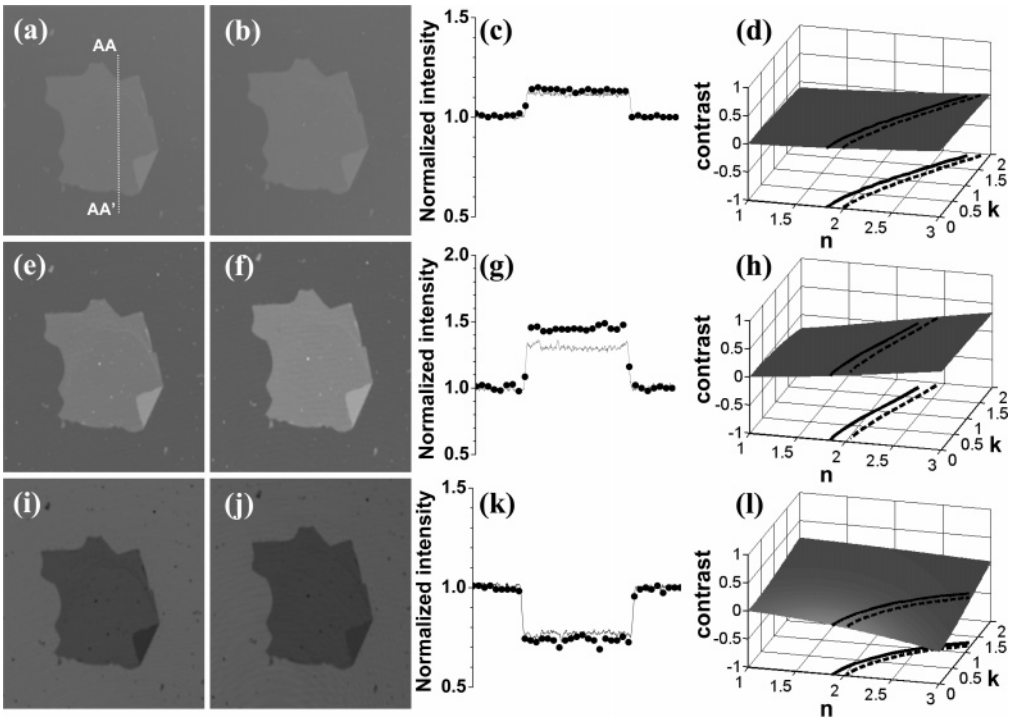

Figure 2. Confocal-microscope images of a graphene oxide single sheet with a 72 nm thick silicon nitride intermediate layer at three different excitation wavelengths: 488 nm (a,b), 543 nm (e,f), and 633 nm (i,j), before (a,e,i) and after (b,f,j) thermal treatment. Intensity plot across the 100 μm long section AA−AA′ before (-) and after (●) thermal treatment: 488 nm (c), 543 nm (g), 633 nm (k). Calculated contrast as a function of refractive index, n, and extinction coefficient, k, of the graphene oxide sheets at three different wavelengths: 488 nm (d), 543 nm (h), and 633 nm (l). Contrast values measured from confocal images are included to show the change in optical properties before (solid line) and after (dashed line) thermal treatment.

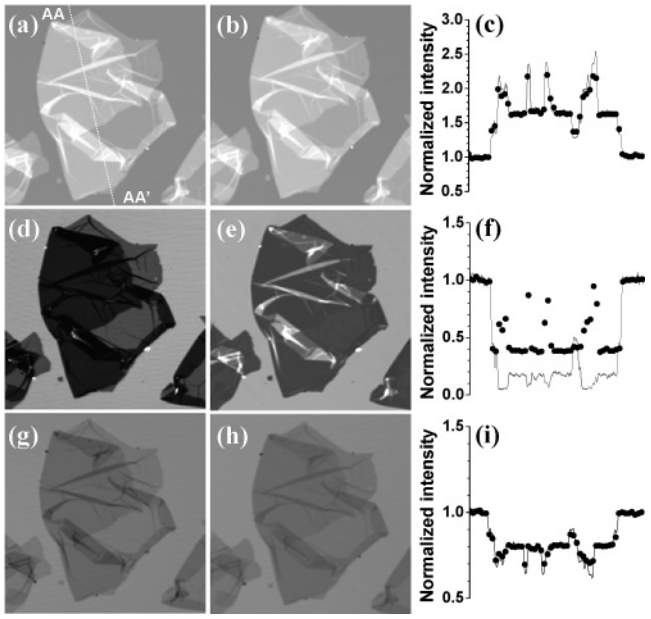

Figure 3. Confocal microscope images of a folded graphene oxide sheet with a 64 nm thick silicon nitride intermediate layer at three different wavelengths: (a,b) 488 nm, (d,e) 543 nm, and (g,h) 633 nm, before (a,d,g) and after (b,e,h) thermal treatment. Intensity plot across the 125 μm long section AA−AA′ before (-) and after (●) thermal treatment for wavelengths of (c) 488 nm, (f) 543 nm, and (i) 633 nm.

reflected intensity is averaged over the angle of incidence, θ, assuming that the incident laser beam has a Gaussian intensity profile. The integration was taken from normal incidence to the maximum incident angle, which is determined by the numerical aperture of the microscope objective and the diameter of the incident beam. For calculation of the reflection amplitudes and phase changes and details on the angular integration, see Supporting Information.

The visibility of the graphene oxide films is characterized in terms of the Michelson contrast[24]

$$\text{contrast} = \frac{R_{\text{material}} - R_{\text{dielectric}}}{R_{\text{material}} + R_{\text{dielectric}}} \tag{3}$$

where R_{material} is the reflected intensity with the material and $R_{\text{dielectric}}$ is the intensity without the material. If the value of the contrast is zero, the material is not detectable; if the value is between 0 and −1, the material appears darker than the substrate; and if it is between 0 and +1, the material is brighter than the substrate.

Silicon dioxide and silicon nitride are commonly deposited on silicon and are thus good candidate dielectrics for enhancing the contrast of thin layers. Their suitability can be determined by calculating the expected contrast as a function of the incident wavelength and of the dielectric film thickness. We consider silicon dioxide deposited by a wet thermal oxidation method and silicon nitride deposited by a stoichiometric growth method, as described in Supporting Information. Figure 1b shows the measured indices of refraction for these two films. Both dielectrics have negligible extinction coefficients. On the basis of these optical properties, the contrast was calculated, assuming as a starting point

Table 1. Layer Thicknesses Measured by AFM

number of layers	thickness before thermal treatment	thickness after thermal treatment
1	1.25 ± 0.08 nm	1.31 ± 0.10 nm
2	2.23 ± 0.11 nm	1.97 ± 0.08 nm
3	3.21 ± 0.21 nm	2.79 ± 0.14 nm
4	4.26 ± 0.25 nm	3.28 ± 0.06 nm

that the graphene oxide layer has $n = 2$, $k = 0$, and $d = 1$ nm. Results for the silicon dioxide layer are shown in Figure 1c-1,c-2. The contrast oscillates slightly around zero with a period that increases with the wavelength of the incident light. Calculated contrast for the silicon nitride intermediate layer is shown in Figure 1d-1,d-2. Compared to the silicon dioxide case, the contrast oscillates at a higher frequency as thickness increases with significantly higher maxima and significantly lower minima as the thickness increases.

With a silicon nitride substrate, high contrast can be obtained for a wide range of optical properties of the thin sheets. Figure 1e,f shows the change in the contrast as the refractive index and absorption coefficient of the thin layer are changed at optimized dielectric-layer thicknesses and optical wavelengths. These results imply that the use of silicon nitride intermediate layers will be effective not only for detecting thin sheets, but also for fitting their effective optical properties, provided that a narrow band light source, such as a laser, is used for illumination.

To verify this prediction, we prepared silicon wafers coated with 61.2, 63.0, 65.5, 67.7, and 71.9 nm of silicon nitride. The thicknesses were measured by spectroscopic ellipsometry and were found to have a variation of approximately 9% across a 4-inch wafer. Figure 2 shows confocal microscope images of a single layer of graphene oxide deposited on the 72 nm thick silicon nitride substrate. As expected, the contrast changes depending on the wavelength of the incident light. The normalized intensity profiles of a graphene oxide sheet, measured at the same cross section before and after thermal treatment, clearly differ, as shown in Figure 2c,g,k. When the sheet thickness was checked by scanning the same region by AFM, no significant change of the thickness of the material was detected, implying that the effective optical properties of the material have been changed.

Figure 2d,h,l shows the calculated contrast, as defined in eq 1, as a function of the effective optical properties of the material layer. Two lines of contrast, before and after thermal treatment, are drawn on the surface and are projected on the plane of optical properties of the material layer. (Details of how experimental contrast is determined are given in Supporting Information.) Although the lines clearly show that the effective optical properties have changed due to the

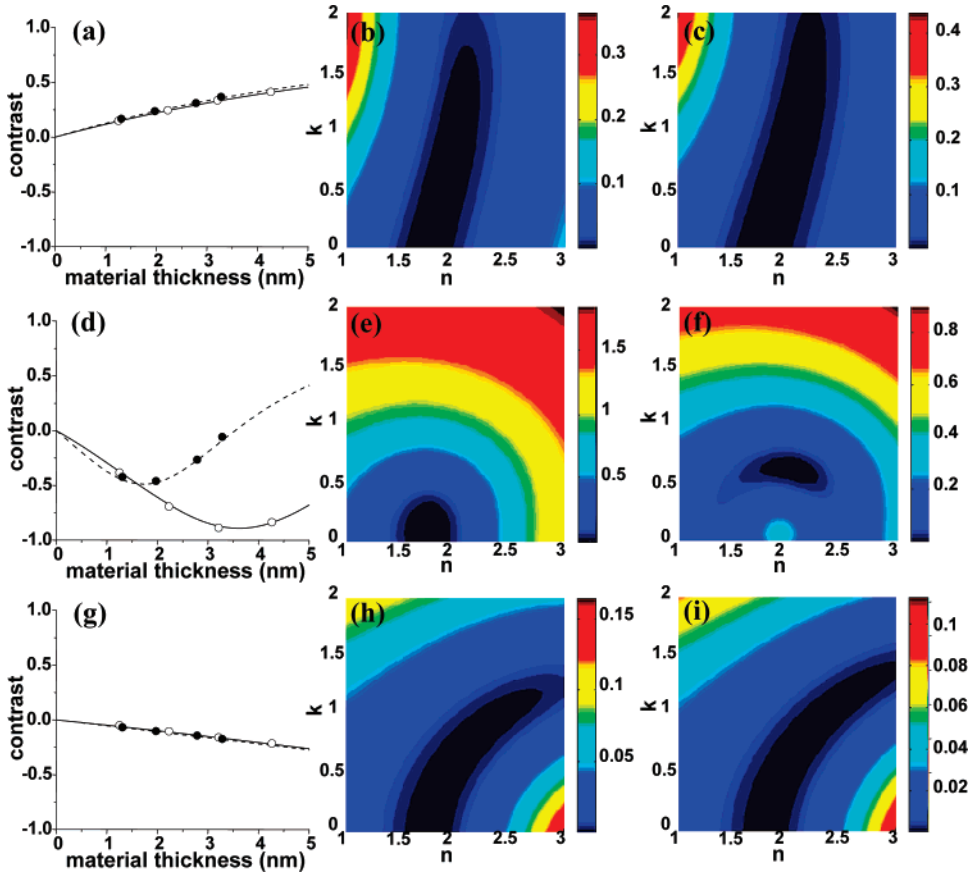

Figure 4. Measured contrast vs thickness of graphene oxide, before (○) and after (●) thermal treatment, and calculated contrast before (solid line) and after (dashed line) thermal treatment for wavelengths of 488 nm (a), 543 nm (d), and 633 nm (g). Contour map of the mean square error between the measured and the calculated contrast for wavelengths of (b,c) 488 nm, (e,f) 543 nm, and (h,i) 633 nm, before (b,e,h) and after (c,f,i) thermal treatment.

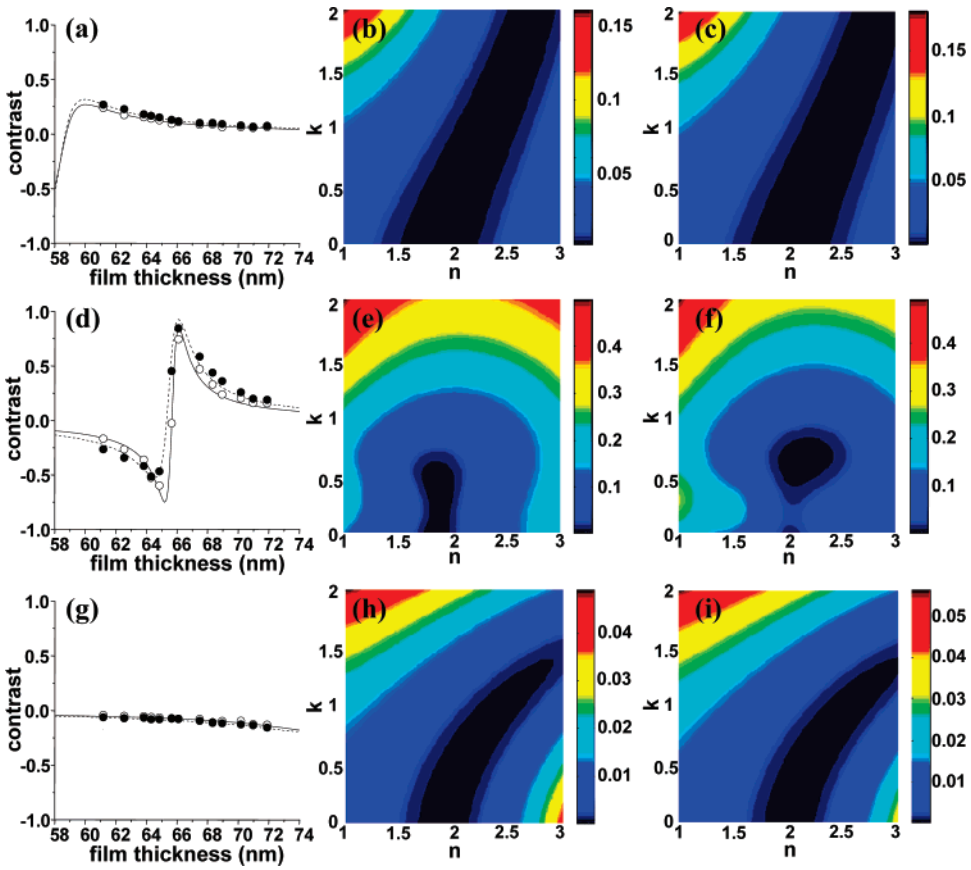

Figure 5. Measured contrast vs thickness of intermediate silicon nitride film before (◯) and after (●) thermal treatment and calculated contrast before (solid line) and after (dashed line) thermal treatment at wavelengths of 488 nm (a), 543 nm (d), and 633 nm (g). Contour map of the mean square error between the measured and the calculated contrast for wavelengths of (b,c) 488 nm, (e,f) 543 nm, and (h,i) 633 nm, before (b,e,h) and after (c,f,i) thermal treatment.

thermal treatment, they do not provide sufficient information to give values of n and k. We therefore systematically investigated the dependence of the contrast on graphene oxide layer thickness, dielectric layer thickness, and optical wavelength and fit the results to theoretical calculations.

Figure 3 shows images of graphene oxide sheets with folded structures on the 64 nm thick silicon nitride layer. The number of graphene oxide layers can be determined by evaluating the folds in the sheets. Up to four layers of a folded graphene oxide sheet can be identified in the section AA−AA′. For an incident wavelength of 543 nm, very large contrast changes result from thermal treatment of the material. Because the contrast change is related to the effective optical properties and the thickness of the material layer, the thickness was measured by AFM before and after the thermal treatment. The results, given in Table 1, show that the thicknesses of multiple layers of graphene oxide are reduced after the thermal treatment with the decrement becoming larger as the number of layers increases. This suggests a decrease in the thickness of intercalated water layers,[25] an important issue for studying multilayer stacks of graphene oxide.[26,27]

In Figure 4a,d,g, the measured and calculated contrasts are shown as a function of the measured graphene oxide thickness. The best fit was found by minimizing the mean square error between the measured and calculated contrast:

$$\text{mean square error} = \sum_{i=1}^{N} (\text{measured contrast}_i - \text{calculated contrast}_i)^2/N \quad (4)$$

where N is the number of data points. The adjustable parameters are the optical constants (n and k) of the material layer; the thickness of the material was assumed to be 1 nm (corresponding to thicknesses measured by AFM). In Figure 4b,c,e,f,h,i, the mean square error is shown on the plane of optical properties of the material layer. The mean square errors for incident wavelengths of 488 and 633 nm do not have a single minimum in the plane of optical properties, but the 543 nm result has a localized minimum, clearly showing that both the effective extinction coefficient and the index of refraction increased with the thermal treatment. We thus suggest that the thermal treatment has partially reduced the graphene oxide sheet, increasing both n and k toward the values for pristine graphene.

In Figure 5a,d,g, contrasts measured from substrates with different silicon nitride thicknesses are shown, along with calculated values. The fitting results again show that the

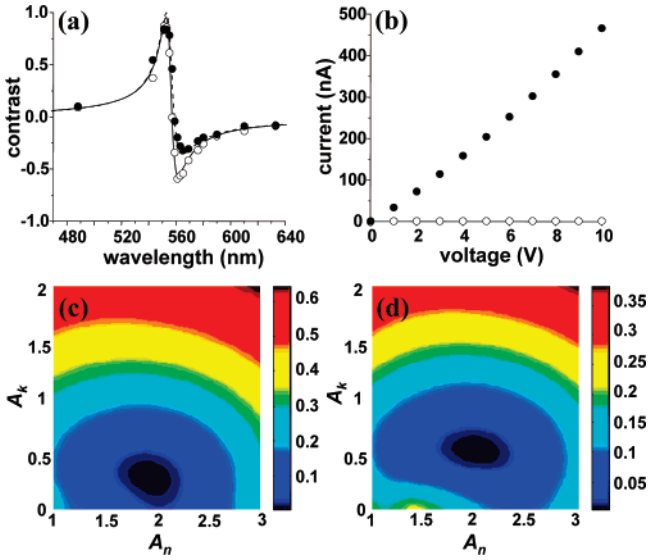

Figure 6. Measured contrast vs wavelength of incident light before (○) and after (●) thermal treatment and calculated contrast before (solid line) and after (dashed line) thermal treatment (a). Current vs voltage for a single graphene oxide sheet before (○) and after (●) thermal treatment (b). Contour map of the mean square error between the measured and the calculated contrast before (c) and after (d) thermal treatment. A_n and A_k are coefficients of the Cauchy functions, $n = A_n + B_n/\lambda^2$ and $k = A_k + B_k/\lambda^2$. The constant values B_n and B_k are assumed to be 3000 and 1500, respectively.

effective index of refraction and extinction coefficient both increased as a result of the thermal treatment (see Figure 5e,f).

We also investigated the effect on the contrast of changing the optical wavelength for a fixed dielectric-layer thickness of 67 nm by performing confocal microscope measurements with a continuously tunable light source. In Figure 6a, the measured and calculated contrast values are shown at different wavelengths. In this case, we have observed contrasts higher than 0.8, which correspond to reflection from the graphene oxide layer 12 times higher than from the bare substrate. To fit the measured data, the effective optical properties are assumed to obey Cauchy functions: $n = A_n + B_n/\lambda^2$ and $k = A_k + B_k/\lambda^2$, with constants B_n and B_k taken to be 3000 and 1500, respectively.[28] The results indicate that that A_n increases from 2.0 ± 0.2 to 2.1 ± 0.2 and A_k from 0.3 ± 0.1 to 0.6 ± 0.1. With the aforementioned values for B_n and B_k, the values of n before and after thermal treatment are 2.0 and 2.1, and the values of k are 0.30 and 0.55, respectively, all at a wavelength of 633 nm. To show that these optical changes are related to physical changes in the material, we have performed transport measurements on the single graphene oxide sheets before and after thermal treatment. As shown in Figure 6b, it was found that the untreated material was electrically insulating and became conductive after thermal treatment.

We also performed preliminary investigations of the effective optical properties of graphene sheets on the same substrates. The thickness of graphene layers were measured in several locations by AFM, and confocal microscope images were acquired for excitation wavelengths of 488, 543, and 633 nm. The relation between the contrast and thickness

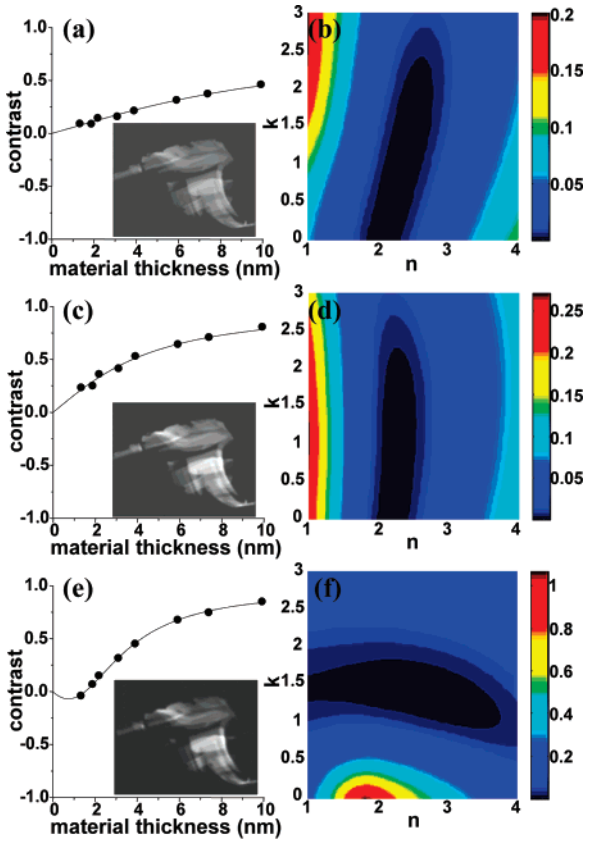

Figure 7. Measured contrast vs thickness of graphene (points) and calculated contrast (lines) at three different excitation wavelengths: 488 nm (a), 543 nm (c), and 633 nm (e). Confocal microscope images at each wavelength (insets). Contour map of the mean square error between the measured and the calculated contrast for wavelengths of (b) 488 nm, (d) 543 nm, and (f) 633 nm.

of deposited graphene was thus obtained and are shown in Figure 7a,c,e. In this case, measurement errors are primarily associated with the uncertainty of the thicknesses determined by AFM. In Figure 7b,d,f, the mean square error is shown; it is minimum for $n \sim 2.5$ and $k \sim 1.3$. These values are significantly higher than those for the thermally treated graphene oxide sheet, but lower than the values reported in the literature for bulk graphite.[29]

In conclusion, it has been shown that a single layer of graphene oxide can readily be identified with optical microscopy by use of a properly designed substrate. The contrast between the sheet and the bare substrate depends on the thickness and optical properties of an intermediate dielectric layer, as was confirmed by confocal microscope measurements. We compared the measured contrast with detailed calculations for graphene oxide layers before and after heating in vacuum. The results suggest that as a consequence of the thermal treatment, both the effective index of refraction and the effective extinction coefficient increase. Further optimization of the contrast should be possible, for example, by using narrower bandwidth light sources, leading to more precise determination of effective optical properties. The method we have demonstrated should be applicable to thin layers of a wide variety of materials, allowing for their rapid imaging and optical characterization.

Acknowledgment. We gratefully acknowledge support from the National Science Foundation (CMS-0510212), the Naval Research Laboratory (No. N00173-04-2-C003), and the DARPA Center on Nanoscale Science and Technology for Integrated Micro/NanoElectromechanical Transducers (iMINT) (Award No. HR0011-06-1-0048). We appreciate assistance by W. Russin (confocal microscopy) and M. Takita (deposition of graphene platelets onto silicon nitride substrates). Work at the Center for Nanoscale Materials was supported by the U.S. Department of Energy, Office of Science, Office of Basic Energy Sciences, under Contract No. DE-AC02-06CH11357. We thank D. Gosztola for technical assistance with variable-wavelength confocal microscopy.

Supporting Information Available: Experimental procedure, calculation of the contrast, comparison of dielectric layers, and uncertainty of optimized optical properties. This material is available free of charge via the Internet at http://pubs.acs.org.

References

(1) Novoselov, K. S.; Geim, A. K.; Morozov, S. V.; Jiang, D.; Zhang, Y.; Dubonos, S. V.; Grigorieva, I. V.; Firsov, A. A. *Science* **2004**, *306*, 666.
(2) Novoselov, K. S.; Jiang, D.; Schedin, F.; Booth, T. J.; Khotkevich, V. V.; Morozov, S. V.; Geim, A. K. *Proc. Natl. Acad. Sci. U.S.A.* **2005**, *102*, 10451.
(3) Piner, R. D.; Xu, T. T.; Fisher, F. T.; Qiao, Y.; Ruoff, R. S. *Langmuir* **2003**, *19*, 7995.
(4) Ding, W.; Dikin, D. A.; Chen, X.; Piner, R. D.; Ruoff, R. S.; Zussman, E.; Wang, X.; Li, X. *J. Appl. Phys.* **2005**, *98*, 014905.
(5) Zahn, Q.; Leger, J. R. *Appl. Opt.* **2002**, *41*, 4443.
(6) Beaglehole, D. *Rev. Sci. Instrum.* **1988**, *59*, 2557.
(7) Jung, I.; Piner, R.; Dikin D.; Stankovich, S.; Ruoff, R. S.; Hausner M. APS Meeting 2006, March 13−17, Baltimore, MD, (Abstract ID: BAPS.2006.MAR.D35.12, http://meetings.aps.org/link/BAPS.2006.MAR.D35.12).
(8) Jung, I.; Piner, R.; Dikin, D.; Stankovich, S.; Watcharotone, S.; Ruoff, R. S. APS Meeting 2007, March 5−9, Denver, CO, (Abstract ID: BAPS.2007.MAR.L28.13, http://meetings.aps.org/link/BAPS.2007.MAR.L28.13).
(9) Zernike, F. *Physica* **1942**, *9*, 686.
(10) Zernike, F. *Physica* **1942**, *9*, 974.
(11) Lambacher, A.; Fromherz, P. *Appl. Phys. A* **1996**, *63*, 207.
(12) Kiessling, V.; Tamm, L. K. *Biophys. J.* **2003**, *84*, 408.
(13) Abergel, D. S. L.; Russell, A.; Fal'ko, V. I. *Appl. Phys. Lett.* **2007**, *91*, 063125.
(14) Roddaro, S.; Pingue, P.; Piazza, V.; Pellegrini, V.; Beltram, F. *Nano Lett.* **2007**, *7*, 2707.
(15) Blake, P.; Novoselov, K. S.; Castro Neto, A. H.; Jiang, D.; Yang, R.; Booth, T. J.; Geim, A. K.; Hill, E. W. *Appl. Phys. Lett.* **2007**, *91*, 063124.
(16) Casiraghi, C.; Hartschuh, A.; Lidorikis, E.; Qian, H.; Harutyunyan, H.; Gokus, T.; Novoselov, K. S.; Ferrari, A. C. *Nano Lett.* **2007**, *7*, 2711.
(17) Ni, Z. H.; Wang, H. M.; Kasmin, J.; Fan, H. M.; Yu, T.; Wu, Y. H.; Feng, Y. P.; Shen, Z. X. *Nano Lett.* **2007**, *7*, 2758.
(18) Stankovich, S.; Piner, R. D.; Chen, X.; Wu, N.; Nguyen, S. T.; Ruoff, R. S. *J. Mat. Chem.* **2006**, *16*, 155.
(19) Hirata, M.; Gotou, T.; Horiuchi, S.; Fujiwara, M.; Ohba, M. *Carbon* **2004**, *42*, 2929.
(20) Stankovich, S.; Dikin, D. A.; Dommett, G. H. B.; Kohlhaas, K. M.; Zimney, E. J.; Stach, E. A.; Piner, R. D.; Nguyen, S. T.; Ruoff, R. S. *Nature* **2006**, *42*, 282.
(21) Ward, L. *The Optical Constants of Bulk Materials and Films*; Institute of Physics Publishing: Philadelphia, PA, 1994.
(22) Macleod, H. A. *Thin-film optical filters*; American Elsevier Publishing Company Inc.: New York, 1969.
(23) Möller, K. D. *Optics*; University Science Books: Mill Valley, CA, 1988.
(24) Michelson, A. *Studies in Optics*; University of Chicago Press: Chicago, IL, 1927.
(25) The thermal treatment changes the chemistry of the graphene oxide sheets, reducing the number of oxygen bonds. It thereby leads to a change in the chemical interaction among the graphene oxide layers and possibly also results in a reduction of their thicknesses. Partial removal of the intercalated water may also affect the measured thicknesses.
(26) Li, J. L.; Chun, J.; Wingreen, N. S.; Car, R.; Aksay, I. A.; Saville, D. A. *Phys. Rev. B* **2005**, *71*, 235412.
(27) Yoshizawa, K.; Yumura, T.; Yamabe, T.; Bandow, S. *J. Am. Chem. Soc.* **2000**, *122*, 11871.
(28) Vaupel, M.; Fuchs, K. Nanofilm Technologie GmbH, Goettingen, Germany. Private communication, 2006.
(29) Djurisic, A. B.; Li, E. H. *J. Appl. Phys.* **1999**, *85*, 7404.

NL0714177